Am J Transl Res 2015;7(9):1588-1601
www.ajtr.org /ISSN:1943-8141/AJTR0010127

Original Article

The effect of synthetic α-tricalcium phosphate on osteogenic differentiation of rat bone mesenchymal stem cells

Jinzhong Liu[1], Liang Zhao[1], Ling Ni[2], Chunyan Qiao[1], Daowei Li[1], Hongchen Sun[1], Zongtao Zhang[2]

[1]Department of Oral Pathology, School of Stomatology, Jilin University, Changchun 130021, China; [2]State Key laboratory Inorganic Synthesis and Preparative Chemistry, Jinlin University, Changchun 130012, China

Received May 11, 2015; Accepted July 9, 2015; Epub September 15, 2015; Published September 30, 2015

Abstract: The reconstruction of large bone defects has been the focus in bone tissue engineering research. By acting as synthetic frameworks for cell growth and tissue formation, biomaterials can play a critical role in bone tissue engineering. Among various biomaterials, calcium phosphate based materials include hydroxyapatite (HA), α-tricalcium phosphate (α-TCP), and β-tricalcium phosphate (β-TCP) are widely used as scaffold materials in bone tissue engineering. However, little is known about the effect of α-TCP alone on the osteogenic differentiation of the BMSCs. To this end, we synthesized α-TCP using a novel co-precipitation method. The synthetic α-TCP was then incubated with rat BMSCs under osteogenic inductive medium culture conditions, followed by the analysis of the mRNA levels of various osteogenesis-related genes, including ALP, Rux2, COL-I, and SP7, using a quantitative RT-PCR method. Following incubation of BMSCs with 20 μg/ml α-TCP, cells reached confluency after 7 days. Additionally, the MTT analysis showed that α-TCP at concentration of 10-20 μg/ml had good biocompatibility with BMSCs, showing no significant inhibition of rat BMSCs proliferation. Furthermore, the synthetic α-TCP (20 μg/ml), when incubated with rat BMSCs in the osteogenic culture medium, increased the mRNA levels of various osteogenesis-related genes, including ALP, Rux2, COL-I, and SP7. Finally, treatment of synthetic α-TCP (20 μg/ml) potentiated calcium nodule formations after incubation with rat BMSCs in osteogenic culture medium for 21 days, as compared with non-treated control. Taken together, the results in the present study suggested that α-TCP alone likely promotes rat BMSCs osteogenic differentiation through up-regulating ALP, Col-I, Runx2, and SP7 gene expression.

Keywords: Co-precipitation, α-tricalcium phosphate, osteogenic differentiation, bone mesenchymal stem cells, tissue engineering

Introduction

The reconstruction of large bone defects caused by trauma, infection, tumors, and congenital malformations has been the focus in bone tissue engineering research. One of the most promising and exciting research developments in bone tissue engineering is to use biomedical materials to facilitate the bone regeneration [1-4]. By acting as synthetic frameworks for cell growth and tissue formation, biomaterials can play a critical role in bone tissue engineering. Ideal bone tissue engineering scaffold materials need to have good biocompatibility, osteoinductivity, and osteoconductivity with similar structure and mechanical properties of natural bones [5]. Furthermore, these biomaterials should be able to form a continuous interface with the bone tissue at the site of implantation, support vascularization, and have matched degradation rate with new bone formation [6-8].

Among various biomaterials, calcium phosphate based materials include hydroxyapatite (HA), α-tricalcium phosphate (α-TCP), and β-tricalcium phosphate (β-TCP) are widely used as scaffold materials in bone tissue engineering [9]. These materials have good bone conductivity and are able to form chemical bonding with the natural bones. In addition to their good structure and mechanical properties, they can promote osteogenesis or new bone formation and biomineralization. Therefore, a few meth-

ods been used to improve the osteoinductive properties of the HA or β-TCP, including the modification of chemical components, inoculation of bone mesenchymal stem cells (BMSCs), and the incorporation of various growth factors such as the transforming growth factor beta (TGF-β) [10], bone morphogenetic protein (BMP) [11, 12], and vascular endothelial growth factor (VEGF) [13, 14]. However, these methods unfortunately resulted in only marginal improvement in bone tissue regeneration likely due to the following two reasons. First, the HA and β-TCP are chemically stable, so that a limited amount of genes or biologically active factors can be carried physically or chemically. Second, the degradation rate of HA and β-TCP is difficult to control and is hard to match with the formation rate of new bones [15-18].

Importantly, α-TCP also has good biodegradability, biocompatibility, and osteoinductivity. The solubility and/or absorption rate of α-TCP are higher than those of β-TCP [19-21]. The degradation products of α-TCP are rapidly absorbed and replaced in the bodies [21]. Given that the degradation of calcium phosphate material generated Ca^{2+}, PO_4^{3-}, which were substrates required by osteoblast differentiation and bone matrix mineralization [7, 22, 23], it is likely that α-TCP alone may promote the osteogenic differentiation of the BMSCs.

Various methods have been developed to synthesize tricalcium phosphate including wet-chemical method [24, 25], solid-state process [26, 27], and microwave irradiation [28, 29]. The most conventional method for α-TCP preparation procedure is the co-precipitation method, which is described as follows. CaH_2PO_4 and $CaCO_3$ are mixed at the molar ratio of 2:1, followed by calcination at 1250°C (or higher) for a certain time period. The final product is then obtained after cooling to the room temperature [30]. However, synthesis of a pure α-TCP by this method often requires a close control of many parameters such as, temperature, due to the different sources of raw materials. For example, studies have reported various sintering temperature ranging from 1200°C-1700°C in order to produce substantially pure α-TCP, which is stable at room temperature [31, 32].

Therefore, in order to examine the effect of α-TCP on the osteogenic differentiation of the BMSCs, we first developed a novel co-precipitation method using calcium nitrate [$Ca(NO_3)_2 \cdot 4H_2O$)], diammonium phosphate [$(NH4)_2HPO_4$], bicarbonate [NH_4HCO_3], and ammonia [NH_3] to prepare α-TCP. The prepared α-TCP product was further characterized by x-ray diffraction analysis (XRD), scanning electron microscopy (SEM), transmission electron microscopy (TEM), and BET surface area analysis. The synthetic α-TCP was then incubated with rat BMSCs under osteogenic inductive medium culture conditions, followed by the analysis of the mRNA levels of various osteogenesis-related genes, including ALP, Rux2, COL-I, and SP7, using a quantitative RT-PCR method.

Materials and methods

Materials and instruments

Analytical grade (A.R.) calcium nitrate [$Ca(NO_3)_2 \cdot 4H_2O$)], diammonium phosphate [$(NH4)_2HPO_4$], bicarbonate [NH_4HCO_3], and Ammonia [NH_3], were used to prepare α–TCP. These reagents were all purchased from Sinopharm Group Co Ltd, China. Magnetic stirrer with heating plates (HJ-6) was purchased from Ronghua Instrument (Jiangsu, China). Programmable high temperature muffle furnace was purchased from Hangzhou Blue Sky Laboratory Instrument (Hangzhou, China). Magnetic pH meter (PHS-3C) was purchased from Shanghai Precision & Scientific Instrument (Shanghai, China). Water circulating vacuum pump was purchased from Yuhua Instrument (Gongyi, China). Electric heating and drying oven was purchased from Sumsung Experimental Instrument (Shanghai, China).

Preparation of α-TCP

α -TCP was prepared by using a co-precipitation method developed in our lab. Briefly, the $Ca(NO_3)_2 \cdot 4H_2O$ and $(NH_4)_2HPO_4$ were used to provide calcium source and phosphorus source, respectively, to prepare precursors rapidly. $Ca(NO_3)_2 \cdot 4H_2O$ was slowly dropped to the mixture of $(NH_4)_2HPO_4$ and NH_4HCO_3 solution under vigorous stirring at 37°C. The Ca/P molar ratio was fixed at 1.5:1. The pH was adjusted to 7.5 with 1 mol/L of aqueous ammonia solution. A suspension was obtained after 1 h stirring. The suspension then underwent vacuum filtration and was washed with water and ethanol, three times each. The filter cake (collected solid) was dried in a dish in the heating and drying oven at

80°C. After drying, the sample was placed in a muffle furnace and was calcined at 1280°C for 2 h, followed by cooling to room temperature.

X-ray diffraction analysis

To determine the crystalline phases, X-ray diffraction (XRD) were measured in a Rigaku D/MAX-2550 X-ray powder diffractometer (Japan) with CuKα (λ = 0.15418 nm) radiation and operating at 50 kV and 200 mA. The scanning range was from 10o to 80o with a rate of 10o/min. Crystalline phases detected in the patterns were identified by comparison to the standard spectrum from the ICDD-PDF (International Center for Diffraction Data-Powder Diffraction Files).

Scanning electron microscopy

The product morphology and particle size was characterized by SEM (JSM-6700F scanning electron microscope, Japan). The sample powder was directly placed onto the sample holder with conductive coating. Excess powder was removed. The sample was treated by desiccation and spray-gold, and was observed after 80 seconds. The accelerating voltage was set at 50 kV.

Transmission electron microscopy

The product morphology and particle size was also characterized by TEM (JEM-2100F transmission electron microscope, Japan). Sample was treated with ultrasonic dispersion in ethanol first, followed by observation on a copper mesh. The accelerating voltage was set at 200 kV.

BET surface area analysis

The product specific surface area was determined by measuring nitrogen adsorption-desorption isotherm with a Micromeritics ASAP2020 apparatus.

Preparation and culture of rat bone mesenchymal stem cells

For isolation of rat BMSCs, tibias and femurs were dissected from adult Sprague-Dawley rat (~200 g; Experimental Animal Center of Jilin University), washed with L-DMEM (DMEM media with L-glutamine). Both epiphyseal ends were then cut to expose the marrow cavity. L-DMEM medium was used to flush the marrow cavity and total fluid was collected. The fluid was subjected to density gradient centrifugation and adherence separation method. Bone marrow suspensions were centrifuged in 15 mL centrifuge tube, 1000 rpm at room temperature for 3-5 min. After centrifugation, the pellet was gently pipetted with 5 mL cell culture medium containing 10% fetal bovine serum. The resulting single cell suspension (2×10^4 cells/flask) was inoculated into 25 mL flasks, and cultured in 37°C, 5% CO_2 humidified incubator. The cell culture medium was changed every 3 days. When the cells reach to 80-90% confluency in flask, they were harvested, replated on 25 ml plastic flask, and cultured to next confluence. Cell morphology and growth were observed under an inverted microscope.

MTT assay

The relative cell growth rate was determined by using MTT assay. Briefly, α-TCP was diluted in cell culture medium to concentrations of 10 μg/ml, 20 μg/ml, 50 μg/ml, 100 μg/ml, and 200 μg/ml, followed by adding into the BMSCs cell culture medium. The negative control group was added 200 μl cell culture medium only. After 1 day, 3 days, 5 days, or 10 days of incubation, the cells were then incubated with 20 μl MTT solution for 4 hr and the cells were solubilized in 150 μl dimethyl sulfoxide (DMSO). The absorbance was measured at a wavelength of 570 nm with a spectrophotometer (Molecular Devices, Silicon Valley, CA, USA). The relative growth rate (RGR) was calculated as RGR = (OD_{exp} Mean/OD_{ctl} Mean) ×100%. The cell morphology and growth status were also observed during incubation under an inverted fluorescence microscope.

Real-time PCR analysis

Total RNA from BMSCs following 3 days, 7 days, or 14 days of incubation in osteogenic culture medium was extracted by TRIZOL Reagent (Invitrogen) according to the manufacturer's instructions. Subsequently, 5 μg of total RNA was converted into cDNA by using Moloney-murine leukemia virus (M-MLV) Superscript II reverse transcriptase (Promega) and random primers (Oligo dT_{18}; Promega). For real-time quantitative RT-PCR., reactions were performed and monitored using an ABI Prism 7700 Sequence Detection System (Applied Biosystems, Rotkreuz, Switzerland). In the same reaction, cDNA samples were analyzed both for the gene of interest and the reference gene

Table 1. Primer sequences for PCR

Gene	GenBank Accession	Sequences of probes	Length (bp)	Product (bP)
Actb	NM_007393.3	F: 5'-CATCCGTAAAGACCTCTATGCCAAC-3'	25	171
		R: 5'-ATGGAGCCACCGATCCACA-3'	19	
Runx2	NM_001145920.1	F: 5'-GCACAAACATGGCCAGATTCA-3'	21	126
		R: 5'-AAGCCATGGTGCCCGTTAG-3'	19	
Sp7	NM_130458.3	F: 5'-AAGTTATGATGACGGGTCAGGTACA-3'	25	129
		5'-AGAAATCTACGAGCAAGGTCTCCAC-3'	25	
Col1	NM_007742.3	F: 5'-GACATGTTCAGCTTTGTGGACCTC-3'	22	119
		R: 5'-GGGACCCTTAGGCCATTGTGTA-3'	25	
Alp	NM_007431.2	F: 5'-CTCAACACCAATGTAGCCAAGAATG-3'	25	75
		R: 5'-GGCAGCGGTTACTGTGGAGA-3'	20	

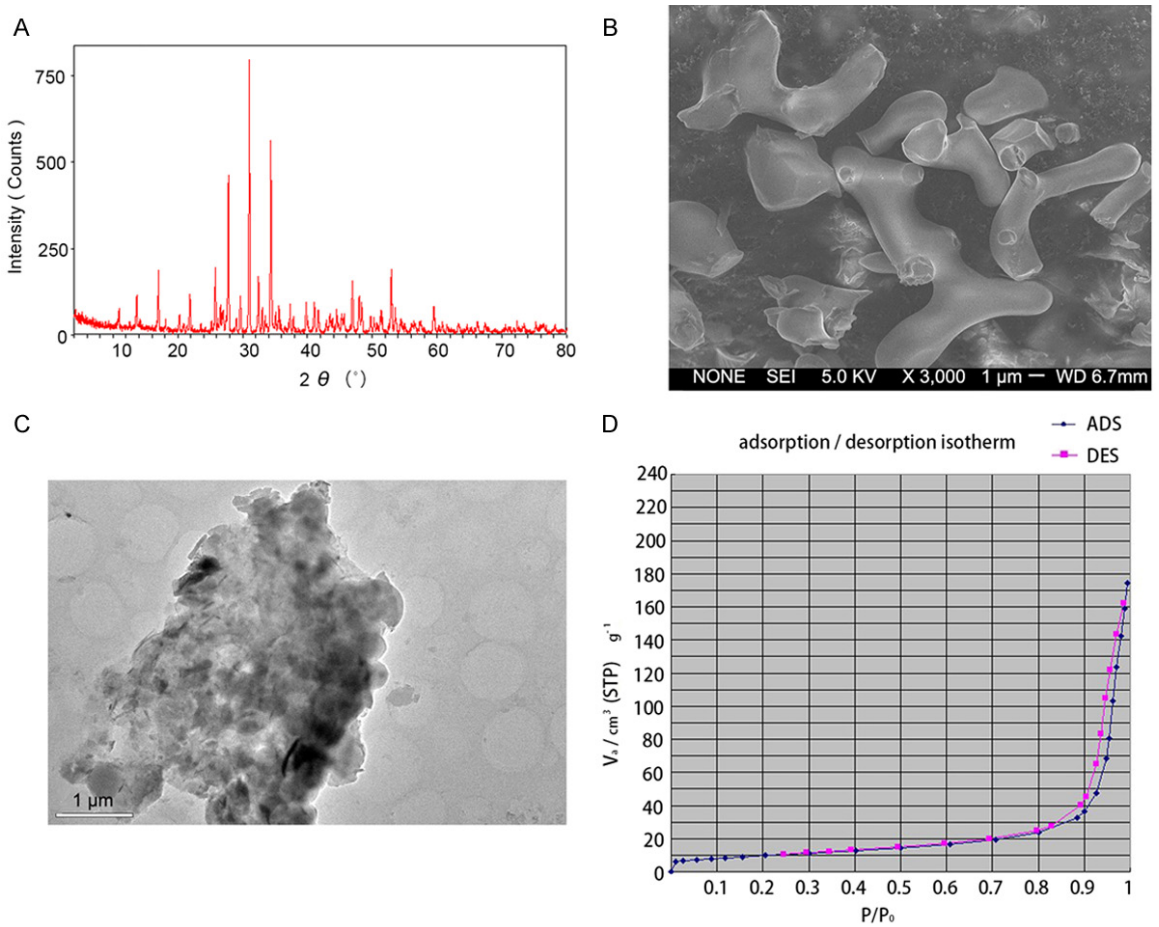

Figure 1. Characterization of synthetic α-TCP product (A) XRD spectrum of α-TCP, (B) SEM image of the macro-architecture of synthetic α-TCP product, (C) TEM image of the prepared α-TCP product, and (D) the nitrogen adsorption and desorption measurements of the prepared α-TCP product. *Blue dots* represent adsorption curve. *Pink dots* represent desorption curve. The α-TCP particles were mostly crystallized in irregular stick-like or peanut-like shapes, with an average particle size of 3-5 μm.

(β-actin). The probes for β-actin and the genes of interest were fluorescently labeled. The primers used were listed in **Table 1**. Amplification was performed using Premix Taq PCR Kit (TaKaRa), with a PCR program mentioned as below: an initial denaturing step of 30 s at

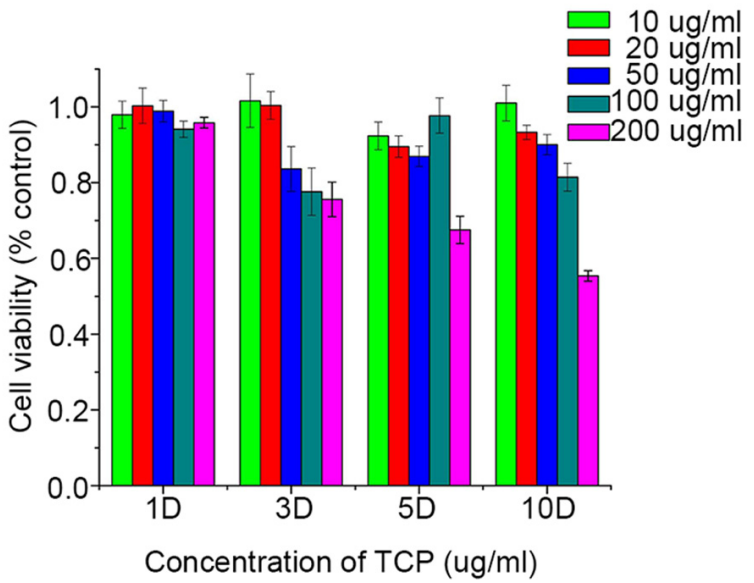

Figure 2. Effects of α-TCP concentrations on the relative cell growth rate of BMSCs. The relative growth rate (RGR) was calculated as RGR = (OD_{exp} Mean/OD_{ctl} Mean) ×100%.

95°C, followed by 40 cycles (95°C for 5 s, 60°C for 30 s, and 72°C for 60 s) and a final extension step for 1 min at 72°C. Expression levels for each gene of interest were calculated by normalizing the quantified mRNA amount to β-actin. Each sample was assessed in three duplicates.

Alizarin red (AZR) staining

AZR staining was used to identify mineralization nodule formation after 21 days in the osteogenic induction culture. Briefly, to obtain 1% AZR staining buffer solution, 1 g AZR was added to Tris-HCl solution, which was made by adding 1 g Tris-HCl was to 100 mL distilled water with the pH adjusted to 7.8 with 0.1 M HCl. Experimental group (α-TCP + BMSCs) and control group (BMSCs only) of cells were incubated for 21 days. After washing twice with PBS buffer, the cells were then fixed with 95% ethanol for 10 min. After washing with PBS buffer again, the cells were incubated with 1% AZR staining buffer solution for 10 min at 37°C. In order to eliminate the non-specific bindings, the cells were incubated in 3 mL PBS solution for 30 min at room temperature and washed gently with PBS solution. The mineralization nodule formation was observed and photographed under an inverted fluorescence microscope. To semi-quantify the mineralization nodule formation, 10% cetylpyridinium chloride in 10 mM Na_2HPO_4 was added to well, followed by shaking for 10 min at room temperature. The absorbance was then measured at a wavelength of 562 nm using a microplate reader.

Data analysis

All values are presented as mean ± standard error of mean. Data were analyzed using t-tests, and analyses of variance (ANOVAs) with repeated measures, where appropriate. Significant ANOVA main and interaction effects were further investigated using Tukey *post hoc* tests, when appropriate. Alpha was set at 0.05.

Results

Characterization of synthetic α-TCP product

We first determined the crystalline phases, and the XRD spectrum of the α-TCP product by the co-precipitation method is shown in **Figure 1A**. We found that the peak intensity of the α-TCP product appeared at 2θ (in degrees) around 20-30° and 40-50°, which is consistent with the standard spectrum of α-TCP. The absence of any other diffraction peaks suggested that the calcined product was pure α-TCP. In addition, the diffraction peaks were high and narrow, indicating that the resulting α-TCP was well crystallized with no other impurities.

Furthermore, we characterized the particle size of synthetic α-TCP using electron microscopy. The SEM images of the α-TCP product by the co-precipitation method are shown in **Figure 1B** and the TEM image of the α-TCP product by the co-precipitation method is shown in **Figure 1C**. Specifically, the α-TCP particles were mostly crystallized in irregular stick-like or peanut-like shapes, with an average particle size of 3-5 μm (**Figure 1B**). Consistent with the SEM analysis, the TEM analysis demonstrated that the particle size of α-TCP was around 3 μm, with porous structures.

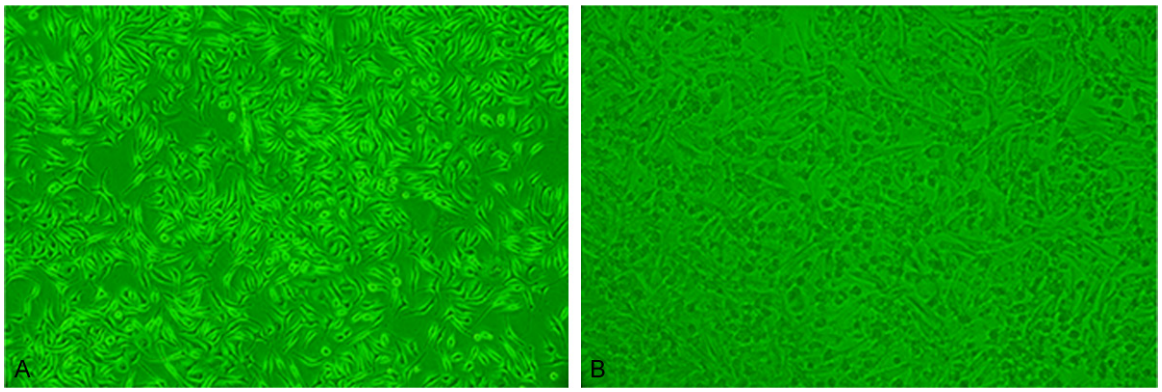

Figure 3. Effects of α-TCP on the morphology of BMSCs culture. After 7 days of culture, cells exhibited homogeneous morphological features (e.g. long spindle shaped) and were arranged in a series, like a whirlpool. A. Non-α-TCP treated control cells. B. α-TCP treated cells reached confluency.

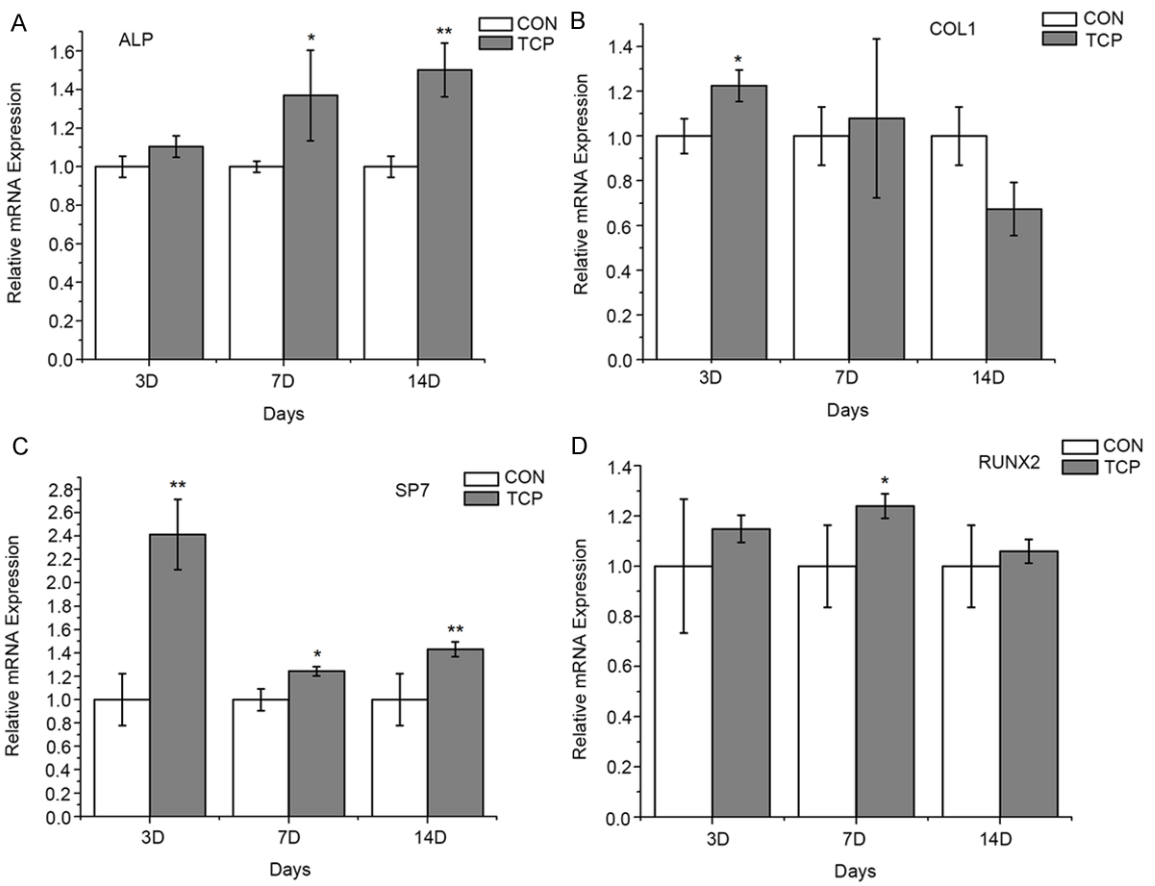

Figure 4. Effects of α-TCP on the expression of (A) ALP, (B) COL-1, (C) SP7, and (D) Runx2 genes after 3, 7, or 14 days of culture. mRNA levels for each gene of interest were calculated by normalizing the quantified mRNA amount to β-actin. *ANOVA simple main effect; $p < 0.05$; **ANOVA simple main effect; $p < 0.01$.

Finally, in order to further confirm the inner architectures, nitrogen adsorption and desorption measurements of the α-TCP product by the co-precipitation method were carried out, and the results are shown in **Figure 1D**. The desorption curve was higher than adsorption curve after $P/P_0 = 0.85$, indicating the presence of mesoporous samples. Furthermore, the desorption curve and adsorption curve were matched together in a lower pressure, suggest-

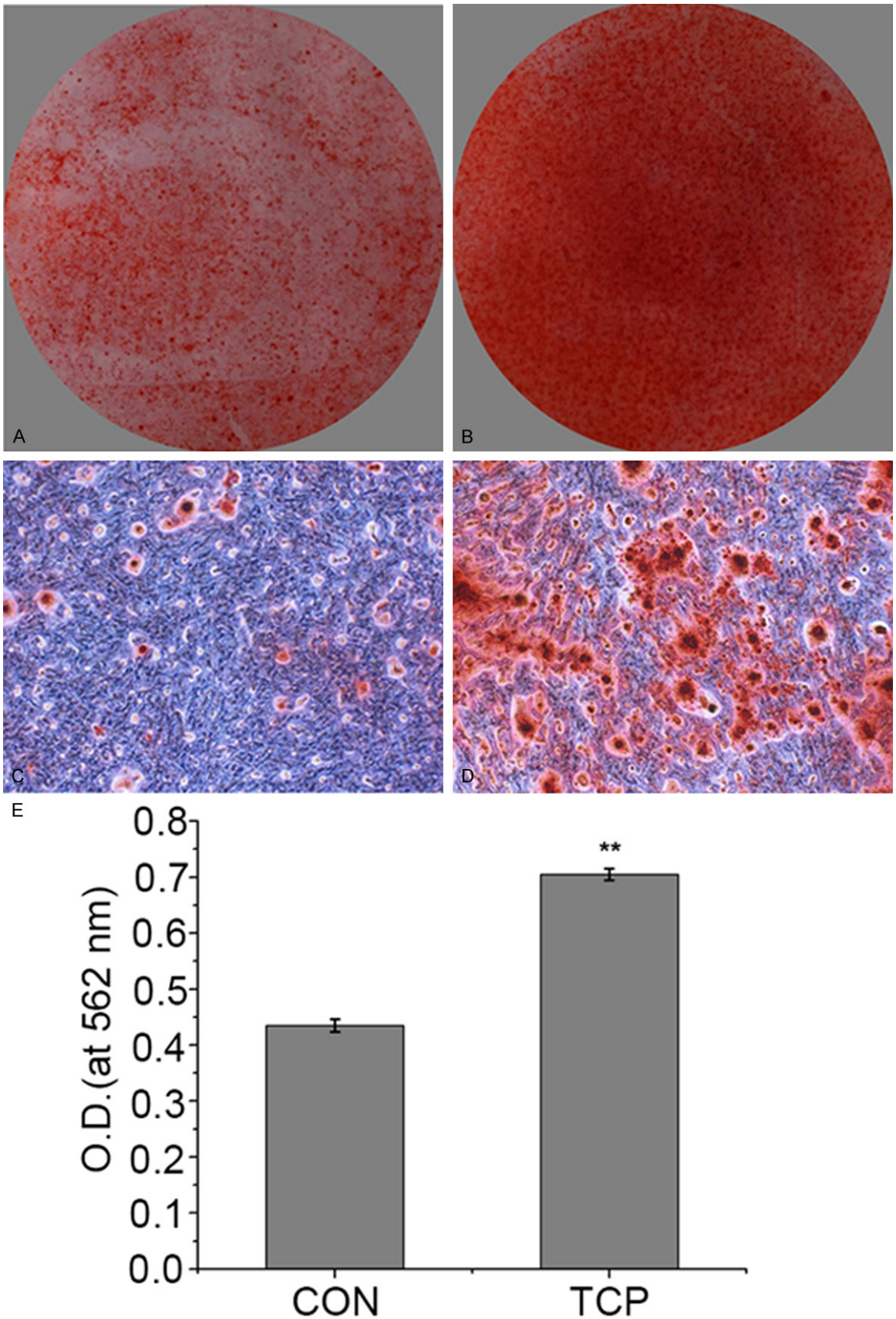
A
B
C
D
E
O.D.(at 562 nm)
0.0
0.1
0.2
0.3
0.4
0.5
0.6
0.7
0.8
**
CON
TCP

Figure 5. Effects of α-TCP on the mineralization nodule formation. Representative images showed red calcium nodule that were visible to naked eyes (A, B) and under the microscope (C, D). Semi-quantitative analysis showed the calcium nodule staining of experimental and control groups (E).

ing that the α-TCP product contained a large number of micropores and a small amount of mesopores.

Effects of α-TCP concentrations on the relative cell growth rate of BMSCs

The results of MTT assay is shown in **Figure 2**. Incubation with α-TCP altered cell proliferation in a concentration dependent manner (all concentration and time main and interaction effects, $F_{(3\text{-}12,\ 10\text{-}30)}$ = 7.18-15.83, p = 0.001-0.03). Specifically, at the concentration of 10 μg/ml or 20 μg/ml, α-TCP did not alter cell proliferation at any time point. However, at the concentration of 50 μg/ml or 100 μg/ml, α-TCP decreased cell proliferation after 3 or 10 days (Tukey test; $p < 0.05$). Furthermore, at the concentration of 200 μg/ml, α-TCP decreased cell proliferation after 3, 5, or 10 days (Tukey test; $p < 0.05$). These results suggested that α-TCP at concentrations higher than 50 μg/ml had a significant effect on cell proliferation rate. Therefore, 20 μg/ml α-TCP was selected for the rest of the experiments in the present study.

Effects of α-TCP on the morphology of BMSCs culture

24 h after inoculation, most of BMSCs adhered to the flask. The morphology of cells was not uniform. Some showed spindle type and some showed polygonal type. The nucleus was large and was found to be located closed to the center or the margin of the cells. Three days later, the number of cells began to increase, and adherent, fibroblast-like cells scattered in a random pattern across the surface of the culture well. Between 7 and 10 days of culture, cells exhibited homogeneous morphological features (e.g. long spindle shaped) and were arranged in a series, like a whirlpool. However, α-TCP (20 μg/ml) treated cells (**Figure 3B**), but not non-α-TCP treated control cells (**Figure 3A**), reached confluency.

Effects of α-TCP on the expression of ALP, COL-1, SP7, and Runx2 genes

After incubation with α-TCP (20 μg/ml), ALP, COL-1, SP7, or Runx2 gene expression was altered in a time-dependent manner (all treatment and time main and interaction effects, $F_{(1\text{-}2,\ 4\text{-}8)}$ = 9.41-16.74, p = 0.0001-0.002). Specifically, ALP gene expression was increased on day 7 (Tukey test; $p < 0.05$) and day 14 (Tukey test; $p < 0.01$), as compared to non-α-TCP treated control group (**Figure 4A**). Furthermore, COL-1 gene expression was initially increased on day 3 (Tukey test; $p < 0.01$), but was decreased on day 14, as compared to non-α-TCP treated control group (**Figure 4B**). Additionally, SP7 gene expression was enhanced on day 3 (Tukey test; $p < 0.01$), day 7 (Tukey test; $p < 0.05$), and day 14 (Tukey test; $p < 0.01$), as compared to non-α-TCP treated control group (**Figure 4C**). Finally, Runx2 gene expression was only increased on day 7 (Tukey test; $p < 0.05$), as compared to non-α-TCP treated control group (**Figure 4D**).

Effects of α-TCP on the mineralization nodule formation

After incubation in osteogenic culture medium for 21 days, both the experimental group (α-TCP + BMSCs) and control group (BMSCs only) showed red calcium nodule that were visible to naked eyes (**Figure 5A** and **5B**) and under the microscope (**Figure 5C** and **5D**). The amount and area of calcium nodule formations in the experimental group were significantly higher than the control group (**Figure 5C** and **5D**). Semi-quantitative analysis confirmed that the calcium nodule staining of experimental group was significantly higher ($t_{(4)}$ = 9.07, $p < 0.01$) than the control group (**Figure 5E**).

Discussion

In the present study, we examined the effect of synthetic α-TCP on the osteogenic differentiation of the rat BMSCs. We have synthesized α-TCP product using a novel co-precipitation method. The results of XRD, SEM, TEM and BET surface analysis indicated that α-TCP was well crystallized with no other impurities, and the average particle size was around 3-5 μm. In addition, the prepared α-TCP product contained a large number of micropores and a small amount of mesopores. Following incubation of BMSCs with 20 μg/ml α-TCP, cells reached confluency after 7 days. Additionally, the MTT analysis showed that α-TCP at concentration of

10-20 μg/ml had good biocompatibility with BMSCs, showing no significant inhibition of rat BMSCs proliferation. Furthermore, using a quantitative RT-PCR method, we demonstrated that the synthetic α-TCP (20 μg/ml), when incubated with rat BMSCs in the osteogenic culture medium, increased the mRNA levels of various osteogenesis-related genes, including ALP, Rux2, COL-I, and SP7. Finally, treatment of synthetic α-TCP (20 μg/ml) potentiated calcium nodule formations after incubation with rat BMSCs in osteogenic culture medium for 21 days, as compared with non-treated control. Taken together, the results in the present study suggested that α-TCP alone likely promotes rat BMSCs osteogenic differentiation through up-regulating ALP, Col-I, Runx2, and SP7 gene expression.

The co-precipitation method, which was utilized in the present study, can improve the robustness of the preparation of α-TCP. Generally, the preparation methods of α-TCP include mechanical and co-precipitation methods. Mechanical method is to mix calcium hydrogen phosphate with calcium carbonate at a certain molar ratio followed by calcining at 1250°C (or higher) and a sudden quenching [33]. Using this method, the calcium hydrogen phosphate and calcium carbonate particles are obtained by grinding. Therefore, the sizes of these particles are large and uneven, and cannot bind tightly. Thus, even under high-temperature, stable α-TCP is still hard to be prepared using the mechanical method. In contrast, the co-precipitation method allows the two components interact closely with a smaller crystal size, thus leading to a sufficient reaction.

Given that the hydration of α-TCP is relatively high, and α-TCP is prone to hydrolysis and conversion into apatite phase with water, α-TCP is commonly utilized as raw material for bone cement powders [34, 35]. However, synthesis of α-TCP often requires strict temperature control. Specifically, tricalcium phosphate has a melting point of 1670°C. It exists three polymorphs, such as β-TCP stable below 1120°C, α-TCP stable between 1120 and 1470°C, and α'-TCP stable above 1470°C. During preparation, α'-TCP can transform into the α-form during cooling. While α-TCP is metastable in a dry environment at room temperature, the crystal transition temperature between β-TCP and α-TCP is 1120-1180°C [36].

Furthermore, an optimal pH of the reaction solution can increase the purity the synthesized α-TCP. A previous study has examined the effects of different pHs on the preparation of α-TCP [37]. Specifically, when the pH was higher than 10.0, it was difficult to obtain α-TCP. However, when the pH was 6.0-8.0, the co-precipitation generated granules of α-TCP [37]. Consistently, in the present study, the pH of the reaction solution was adjusted to 7.5. Subsequent XRD analysis demonstrated that the α-TCP product spectrum was consistent with the standard spectrum, with no other diffraction peaks. The diffraction peaks were high and narrow, indicating that the calcined product was pure with no impurities.

Previous studies have demonstrated that the particle size of β-TCP and the surface properties of β-TCP particles have significant influence on osteoblast function [38]. Specifically, β-TCP particles with diameter greater than 10 μm can inhibit the osteoblast survival rate, osteoblast proliferation and extracellular matrix production by osteoblast, suggesting that the physical properties of the materials may affect the function of osteoblasts. The SEM and TEM analysis showed that the particle size of the synthesized α-TCP was 3-5 μm in the present study. Furthermore, both TEM analysis and nitrogen adsorption experiment confirmed that the α-TCP particles in the present study formed a large amount of micropores and a few mesopores. Such type of synthetic materials with micropores or microspheres allows the delivery of pharmacological agents or gene therapy products to further promote bone regeneration.

When in osteogenic culture *in vitro*, BMSCs mainly go through three distinctive stages, including cell proliferation, differentiation, and mineralization of extracellular matrix [39]. After cells adhere to the flasks, transformed cells will start the proliferation. At proliferation stage, cells begin to form colony, integrate, and grow multiple layers, which is characterized by the transcription and protein expression of alkaline phosphatase (ALP) [40]. During the differentiation stage, the activity of alkaline phosphatase (ALP) and the secretion of collagen type I (Col-I) are increased [41]. BMSCs continue to express

biomarker proteins at different differentiating stages into osteoblasts, such as ALP and Col-I, which are highly expressed in osteoblasts early differentiation, and decrease after the mineralization. During the stage of mineralization of extracellular matrix, ALP level starts to decline after this initial peak. The expression of genes such as osteopontin (OPN), osteocalcin (BGP), and bone sialoprotein (BSP), which are related with hydroxyapatite deposition, start to peak [39, 42]. OPN is the first matrix protein expressed, followed by BSP. Ultimately BGP expression and extracellular matrix calcification occur simultaneously. Thus, the stage of mineralization of extracellular matrix is characterized with the secretion of BGP and the deposition of calcium. During this stage, calcified nodule formations are visible via Alizarin Red staining. The synergistic functions of these matrix proteins ensure the maturation of the extracellular matrix, which will allow the osteoblasts to be embedded to form bone tissues.

In the present study, we demonstrated that the level of ALP mRNA maintained at a higher level from day 3 to day 14 in the α-TCP treated experimental group, indicating a strong osteogenic inductive effect of α-TCP in the early stage of BMSCs differentiation. Bone-specific ALP is considered to be a highly specific marker of the bone-forming activity of osteoblasts, which are mainly distributed on the cell membrane [43, 44]. ALP has a high expression in osteoblast and is the marker of osteoblast maturation [44, 45]. As an early marker of osteoblast differentiation, ALP starts to appear during the formation of the matrix, and reaches the peak level at calcification stage [46]. ALP promotes cell maturation and calcification and plays an important role in bone and tooth formation, metabolism and regeneration [47, 48]. It has been reported that ALP facilitates hard tissue calcification by providing phosphate and removing calcification inhibitors [47]. Specifically, ALP can hydrolyze phosphate ester, so that the local phosphate concentration is increased. Additionally, ALP can hydrolyze ATP, which provides energy for the active transport, and increases the local concentration of calcium or phosphate. Furthermore, ALP can remove pyrophosphate as calcification inhibitor. Finally, ALP has a high affinity with calcium, and could facilitate calcium crystallization with inorganic and promote mineralization [49].

Furthermore, the present study has demonstrated that the level of Col-I mRNA rose in from 3 days to 7 days in the α-TCP treated experimental group, indicating that α-TCP likely promotes the differentiation of BMSCs to osteoblasts. Col-I is the major organic component of the extracellular matrix in bone tissues and is the main component of fibrin, which accounts for over 90% of the organic matrix of bones. It is the template for bone organic matrix, and is critical for the location and growth space of bone mineralization. Col-I is produced by osteoblasts *in vitro* and formed into collagen matrix, which can change the structure of the cell and ultimately form mature bone matrix [50]. The amount and structural stability of Col-I id critical for maintaining the normal structure and functions of bones [51]. Furthermore, as one of the markers of osteoblasts, Col-I can promote BMSCs adhesion, proliferation, and differentiation [52]. In addition, Col-I is also a marker of osteoblast differentiation [53]. It is the scaffold for calcium deposition and cell adhesion. During the process of matrix mineralization, other molecules, such as osteonectin, BGP, OPN, and various growth factors as well as calcium released by matrix vesicles of osteoblasts, will deposit on collagen matrix under the effects of ALP. Additionally, in the present study, we have demonstrated that calcium nodules of BMSCs in α-TCP treated group were stronger than the non-α-TCP treated control group after 21 days incubation with α-TCP. Thus, α-TCP may not only facilitate the osteoblast differentiation, but accelerate the mineralization of the extracellular matrix.

Additionally, the present study has demonstrated that α-TCP treated BMSCs showed significantly higher levels of Runx2/SP7 mRNA after 14 days, as compared to control group, indicating that α-TCP may enhance BMSCs differentiation to mature osteoblasts. Runt-related transcription factor 2 (Runx2) is a bone-specific transcription factor that regulates the expression of several osteoblastic genes [54]. Runx2 knockout mice are lack of bone formation due to the disruption of osteoblast differentiation and maturation [55]. Osx (the human homologue of SP7) is downstream of Runx2, and plays crucial role in the differentiation of osteoblast into mature osteoblasts [56]. Osx knockout can lead to the disruption of the differentiation and maturation of osteoblast [57].

Therefore, Runx2 and Osx regulate osteoblast differentiation and bone formation, by regulating the expression of several osteogenesis-related genes such as ALP, Col-I, BSP, and OCN.

Finally, α-TCP may facilitate osteogenic differentiation by activation of mitogen-activating protease (MAPKs) mediated signaling pathways. Cells differentiation requires the activations of multiple intracellular and extracellular signaling pathways, through which growth factors can regulate cell activity via autocrine or paracrine. MAPKs is critical for converting variety of stimuli to intracellular signaling, and is involved in the regulation of many physiological functions such as cell proliferation, differentiation, inflammation, and apoptosis [58]. Extracellular signal-regulating kinase 1/2 (ERK1/2), a downstream target of MAPK (MEK), is also required for osteoblast differentiation and skeletal development [59, 60]. For instance, activation of MAPKs could stimulate the osteogenic differentiation of MC3T3-E1 cells and human BMSCs [61]. During the maturation process of osteogenic cells, MAPK signaling pathway is regulated by the expression of various osteoblast markers [59]. In the present study, calcium produced by degradation of porous α-TCP materials likely contact with BMSCs, activating MAPKs mediated signaling pathways through calcium activated receptors on the surface of the membrane, thereby reinforcing BMSCs differentiation and achieving excellent osteoinductive effect. Thus, our future work will focus on investigating the mechanisms underlying the effects of α-TCP on facilitating osteogenic differentiation.

In summary, the present study has successfully prepared pure α-TCP using a co-precipitation method with $Ca(NO_3)_2 \cdot 4H_2O$, $(NH4)_2HPO_4$, NH_4HCO_3, and NH_3 as raw materials. This method was more efficient than traditional methods. However, in the present study, the synthesis temperature of α-TCP was about 1280°C. We are currently attempting to decrease the synthesis temperature of α-TCP by using "hydrothermal synthesis" approach under pressurized conditions. Such an approach may decrease the reaction time and allow the synthesis of a large amount of α-TCP conveniently. Furthermore, our research group has already prepared poly (lactic-co-glycolic acid) (PLGA) microspheres containing BMP gene. Our previous study has demonstrated that the BMP gene containing PLGA microspheres achieved excellent results in promoting bone tissue formation [62]. Thus, when coupled with the delivery of gene therapy products, the synthesized α-TCP in this study will likely provide a potential therapeutic tool in bone tissue regeneration.

Acknowledgements

This study was supported by Grants from The fundamental research funds for the Central Universities foundation (NO. JCKY-QKJC29). The National Natural Science Foundation of China (No. 81400488) and Project of the provincial science and Technology Department (No. 20140204018SF).

Disclosure of conflict of interest

None.

Address correspondence to: Hongchen Sun, Department of Oral Pathology, School of Stomatology, Jilin University, No. 1500 Xinhua Road, Changchun 130021, China. E-mail: drhcsun@163.com; Zongtao Zhang, State Key laboratory Inorganic Synthesis and Preparative Chemistry, Jinlin University, No. 2699 Qianjin Street, Changchun 130012, China. E-mail: ztzhangjlu@yeah.net

References

[1] Font Tellado S, Rosado Balmayor E and Van Griensven M. Strategies to engineer tendon/ligament-to-bone interface: Biomaterials, cells and growth factors. Adv Drug Deliv Rev 2015; [Epub ahead of print].

[2] Samorezov JE and Alsberg E. Spatial regulation of controlled bioactive factor delivery for bone tissue engineering. Adv Drug Deliv Rev 2015; 84: 45-57.

[3] Sriram M, Sainitya R, Kalyanaraman V, Dhivya S and Selvamurugan N. Biomaterials mediated microRNA delivery for bone tissue engineering. Int J Biol Macromol 2015; 74C: 404-412.

[4] Fernandez-Yague MA, Abbah SA, McNamara L, Zeugolis DI, Pandit A and Biggs MJ. Biomimetic approaches in bone tissue engineering: Integrating biological and physicomechanical strategies. Adv Drug Deliv Rev 2015; 84: 1-29.

[5] Hutmacher DW. Scaffolds in tissue engineering bone and cartilage. Biomaterials 2000; 21: 2529-2543.

[6] Kinoshita Y and Maeda H. Recent developments of functional scaffolds for craniomaxillofacial bone tissue engineering applications. ScientificWorldJournal 2013; 2013: 863157.

[7] Barrere F, van Blitterswijk CA and de Groot K. Bone regeneration: molecular and cellular interactions with calcium phosphate ceramics. Int J Nanomedicine 2006; 1: 317-332.
[8] Amini AR, Laurencin CT and Nukavarapu SP. Bone tissue engineering: recent advances and challenges. Crit Rev Biomed Eng 2012; 40: 363-408.
[9] Dorozhkin SV and Epple M. Biological and medical significance of calcium phosphates. Angew Chem Int Ed Engl 2002; 41: 3130-3146.
[10] Chen Y, Wang J, Zhu XD, Tang ZR, Yang X, Tan YF, Fan YJ and Zhang XD. Enhanced effect of beta-tricalcium phosphate phase on neovascularization of porous calcium phosphate ceramics: in vitro and in vivo evidence. Acta Biomater 2015; 11: 435-448.
[11] Lu Z, Roohani-Esfahani SI, Li J and Zreiqat H. Synergistic effect of nanomaterials and BMP-2 signalling in inducing osteogenic differentiation of adipose tissue-derived mesenchymal stem cells. Nanomedicine 2015; 11: 219-228.
[12] Zhao J, Hu J, Wang S, Sun X, Xia L, Zhang X, Zhang Z and Jiang X. Combination of beta-TCP and BMP-2 gene-modified bMSCs to heal critical size mandibular defects in rats. Oral Dis 2010; 16: 46-54.
[13] Henrich D, Verboket R, Schaible A, Kontradowitz K, Oppermann E, Brune JC, Nau C, Meier S, Bonig H, Marzi I and Seebach C. Characterization of bone marrow mononuclear cells on biomaterials for bone tissue engineering in vitro. Biomed Res Int 2015; 2015: 762407.
[14] Geiger F, Beverungen M, Lorenz H, Wieland J, Fehr M and Kasten P. Bone Substitute Effect on Vascularization and Bone Remodeling after Application of phVEGF165 Transfected BMSC. J Funct Biomater 2012; 3: 313-326.
[15] Oryan A, Alidadi S, Moshiri A and Maffulli N. Bone regenerative medicine: classic options, novel strategies, and future directions. J Orthop Surg Res 2014; 9: 18.
[16] Calori GM, Mazza E, Colombo M and Ripamonti C. The use of bone-graft substitutes in large bone defects: any specific needs? Injury 2011; 42 Suppl 2: S56-63.
[17] Nandi SK, Roy S, Mukherjee P, Kundu B, De DK and Basu D. Orthopaedic applications of bone graft & graft substitutes: a review. Indian J Med Res 2010; 132: 15-30.
[18] Giannoudis PV, Dinopoulos H and Tsiridis E. Bone substitutes: an update. Injury 2005; 36 Suppl 3: S20-27.
[19] Li Y, Weng W and Tam KC. Novel highly biodegradable biphasic tricalcium phosphates composed of alpha-tricalcium phosphate and beta-tricalcium phosphate. Acta Biomater 2007; 3: 251-254.
[20] Chow LC. Calcium phosphate materials: reactor response. Adv Dent Res 1988; 2: 181-184; discussion 185-186.
[21] Yamada M, Shiota M, Yamashita Y and Kasugai S. Histological and histomorphometrical comparative study of the degradation and osteoconductive characteristics of alpha- and beta-tricalcium phosphate in block grafts. J Biomed Mater Res B Appl Biomater 2007; 82: 139-148.
[22] Ko CL, Chen WC, Chen JC, Wang YH, Shih CJ, Tyan YC, Hung CC and Wang JC. Properties of osteoconductive biomaterials: calcium phosphate cement with different ratios of platelet-rich plasma as identifiers. Mater Sci Eng C Mater Biol Appl 2013; 33: 3537-3544.
[23] Ben-Nissan B. Advances in Calcium Phosphate Biomaterials Preface. Advances in Calcium Phosphate Biomaterials 2014; 2: Ix-Xi.
[24] Pan Y, Huang JL and Shao CY. Preparation of beta-TCP with high thermal stability by solid reaction route. Journal of Materials Science 2003; 38: 1049-1056.
[25] Li ZM, He W, Wang YJ, Zhang XD, Zhao HS, Yan SP and Zhou WJ. A Simple Method to Synthesize Nanocrystalline Hydroxyapatite. Journal of Advanced Materials 2009; 41: 28-32.
[26] Liou SC and Chen SY. Transformation mechanism of different chemically precipitated apatitic precursors into beta-tricalcium phosphate upon calcination. Biomaterials 2002; 23: 4541-4547.
[27] Tas AC, Korkusuz F, Timucin M and Akkas N. An investigation of the chemical synthesis and high-temperature sintering behaviour of calcium hydroxyapatite (HA) and tricalcium phosphate (TCP) bioceramics. J Mater Sci Mater Med 1997; 8: 91-96.
[28] Farzadi A, Solati-Hashjin M, Bakhshi F and Aminian A. Synthesis and characterization of hydroxyapatite/beta-tricalcium phosphate nanocomposites using microwave irradiation. Ceram Int 2011; 37: 65-71.
[29] Sha L, Liu YY, Zhang Q, Hu M and Jiang YS. Microwave-assisted co-precipitation synthesis of high purity beta-tricalcium phosphate crystalline powders. Mater Chem Phys 2011; 129: 1138-1141.
[30] Suvorova EI, Arkharova NA and Buffat PA. Transmission electron microscopy of Ca oxide nano- and microcrystals in alpha-tricalcium phosphate prepared by sintering of beta-tricalcium phosphate. Micron 2009; 40: 563-570.
[31] Morejón-Alonso L, Ferreira OJ, Carrodeguas RG, dos Santos LA. Bioactive composite bone cement based on a-tricalcium phosphate/tricalcium silicate. J Biomed Mater Res B Appl Biomater 2012; 100B: 94-102.

[32] Carrodeguas RG and De Aza S. alpha-Tricalcium phosphate: Synthesis, properties and biomedical applications. Acta Biomaterialia 2011; 7: 3536-3546.
[33] Xu HH and Simon CG Jr. Self-hardening calcium phosphate composite scaffold for bone tissue engineering. JJ Orthop Res 2004; 22: 535-543.
[34] Gandolfi MG, Ciapetti G, Taddei P, Perut F, Tinti A, Cardoso MV, Van Meerbeek B and Prati C. Apatite formation on bioactive calcium-silicate cements for dentistry affects surface topography and human marrow stromal cells proliferation. Dent Mater 2010; 26: 974-992.
[35] Brunner TJ, Bohner M, Dora C, Gerber C and Stark WJ. Comparison of amorphous TCP nanoparticles to micron-sized alpha-TCP as starting materials for calcium phosphate cements. J Biomed Mater Res B Appl Biomater 2007; 83: 400-407.
[36] Cicek G, Aksoy EA, Durucan C and Hasirci N. Alpha-tricalcium phosphate (alpha-TCP): solid state synthesis from different calcium precursors and the hydraulic reactivity. J Mater Sci Mater Med 2011; 22: 809-817.
[37] Yang H and Fu S. Preparation of α-Tricalcium Phosphate by Co-precipitation. Chemistry 2007; 1: 392-395.
[38] Pioletti DP, Takei H, Lin T, Van Landuyt P, Ma QJ, Kwon SY and Sung KL. The effects of calcium phosphate cement particles on osteoblast functions. Biomaterials 2000; 21: 1103-1114.
[39] Huang Z, Nelson ER, Smith RL and Goodman SB. The sequential expression profiles of growth factors from osteoprogenitors [correction of osteroprogenitors] to osteoblasts in vitro. Tissue Eng 2007; 13: 2311-2320.
[40] Aubin JE. Regulation of osteoblast formation and function. Rev Endocr Metab Disord 2001; 2: 81-94.
[41] Quarles LD, Yohay DA, Lever LW, Caton R and Wenstrup RJ. Distinct proliferative and differentiated stages of murine MC3T3-E1 cells in culture: an in vitro model of osteoblast development. J Bone Miner Res 1992; 7: 683-692.
[42] Hoemann CD, El-Gabalawy H and McKee MD. In vitro osteogenesis assays: influence of the primary cell source on alkaline phosphatase activity and mineralization. Pathol Biol (Paris) 2009; 57: 318-323.
[43] Bellows CG, Aubin JE and Heersche JN. Initiation and progression of mineralization of bone nodules formed in vitro: the role of alkaline phosphatase and organic phosphate. Bone Miner 1991; 14: 27-40.
[44] Golub EE, Harrison G, Taylor AG, Camper S and Shapiro IM. The role of alkaline phosphatase in cartilage mineralization. Bone Miner 1992; 17: 273-278.
[45] He G and George A. Dentin matrix protein 1 immobilized on type I collagen fibrils facilitates apatite deposition in vitro. J Biol Chem 2004; 279: 11649-11656.
[46] Kihara T, Oshima A, Hirose M and Ohgushi H. Three-dimensional visualization analysis of in vitro cultured bone fabricated by rat marrow mesenchymal stem cells. Biochem Biophys Res Commun 2004; 316: 943-948.
[47] Orimo H. The mechanism of mineralization and the role of alkaline phosphatase in health and disease. J Nippon Med Sch 2010; 77: 4-12.
[48] Mornet E, Stura E, Lia-Baldini AS, Stigbrand T, Menez A and Le Du MH. Structural evidence for a functional role of human tissue nonspecific alkaline phosphatase in bone mineralization. J Biol Chem 2001; 276: 31171-31178.
[49] Reilly TM, Seldes R, Luchetti W and Brighton CT. Similarities in the phenotypic expression of pericytes and bone cells. Clin Orthop Relat Res 1998; 95-103.
[50] Lian JB and Stein GS. Concepts of osteoblast growth and differentiation: basis for modulation of bone cell development and tissue formation. Crit Rev Oral Biol Med 1992; 3: 269-305.
[51] Hosoi T. Bone and bone related biochemical examinations. Bone and collagen related metabolites. Structure and metabolisms of collagen. Clin Calcium 2006; 16: 971-976.
[52] Liu G, Hu YY, Zhao JN, Wu SJ, Xiong Z and Lu R. Effect of type I collagen on the adhesion, proliferation, and osteoblastic gene expression of bone marrow-derived mesenchymal stem cells. Chin J Traumatol 2004; 7: 358-362.
[53] Wenstrup RJ, Witte DP and Florer JB. Abnormal differentiation in MC3T3-E1 preosteoblasts expressing a dominant-negative type I collagen mutation. Connect Tissue Res 1996; 35: 249-257.
[54] Ducy P, Zhang R, Geoffroy V, Ridall AL and Karsenty G. Osf2/Cbfa1: a transcriptional activator of osteoblast differentiation. Cell 1997; 89: 747-754.
[55] Komori T, Yagi H, Nomura S, Yamaguchi A, Sasaki K, Deguchi K, Shimizu Y, Bronson RT, Gao YH, Inada M, Sato M, Okamoto R, Kitamura Y, Yoshiki S and Kishimoto T. Targeted disruption of Cbfa1 results in a complete lack of bone formation owing to maturational arrest of osteoblasts. Cell 1997; 89: 755-764.
[56] Chiu R, Smith KE, Ma GK, Ma T, Smith RL and Goodman SB. Polymethylmethacrylate particles impair osteoprogenitor viability and expression of osteogenic transcription factors Runx2, osterix, and Dlx5. J Orthop Res 2010; 28: 571-577.

[57] Nakashima K, Zhou X, Kunkel G, Zhang Z, Deng JM, Behringer RR and de Crombrugghe B. The novel zinc finger-containing transcription factor osterix is required for osteoblast differentiation and bone formation. Cell 2002; 108: 17-29.

[58] Don MJ, Lin LC and Chiou WF. Neobavaisoflavone stimulates osteogenesis via p38-mediated up-regulation of transcription factors and osteoid genes expression in MC3T3-E1 cells. Phytomedicine 2012; 19: 551-561.

[59] Ge C, Xiao G, Jiang D and Franceschi RT. Critical role of the extracellular signal-regulated kinase-MAPK pathway in osteoblast differentiation and skeletal development. J Cell Biol 2007; 176: 709-718.

[60] Greenblatt MB, Shim JH, Zou W, Sitara D, Schweitzer M, Hu D, Lotinun S, Sano Y, Baron R, Park JM, Arthur S, Xie M, Schneider MD, Zhai B, Gygi S, Davis R and Glimcher LH. The p38 MAPK pathway is essential for skeletogenesis and bone homeostasis in mice. J Clin Invest 2010; 120: 2457-2473.

[61] Jadlowiec J, Koch H, Zhang X, Campbell PG, Seyedain M and Sfeir C. Phosphophoryn regulates the gene expression and differentiation of NIH3T3, MC3T3-E1, and human mesenchymal stem cells via the integrin/MAPK signaling pathway. J Biol Chem 2004; 279: 53323-53330.

[62] Qiao C, Zhang K, Jin H, Miao L, Shi C, Liu X, Yuan A, Liu J, Li D, Zheng C, Zhang G, Li X, Yang B and Sun H. Using poly(lactic-co-glycolic acid) microspheres to encapsulate plasmid of bone morphogenetic protein 2/polyethylenimine nanoparticles to promote bone formation in vitro and in vivo. Int J Nanomedicine 2013; 8: 2985-2995.